Electrostatic Assembly of Sandwich-Like Ag-C@ZnO-C@Ag-C Hybrid Hollow Microspheres with Excellent High-Rate Lithium Storage Properties

Qingshui Xie[†], Yating Ma[†], Xuanpeng Wang[‡], Deqian Zeng[†], Laisen Wang[†], Liqiang Mai[‡] and Dong-Liang Peng[†]*

[†]*Fujian Key Laboratory of Advanced Materials, Collaborative Innovation Center of Chemistry for Energy Materials, Department of Materials Science and Engineering, College of Materials, Xiamen University, Xiamen 361005, China*

[‡]*State Key Laboratory of Advanced Technology for Materials Synthesis and Processing, WUT-Harvard Joint Nano Key Laboratory, Wuhan University of Technology, Wuhan 430070, China*

Corresponding Author

[*]E-mail: dlpeng@xmu.edu.cn

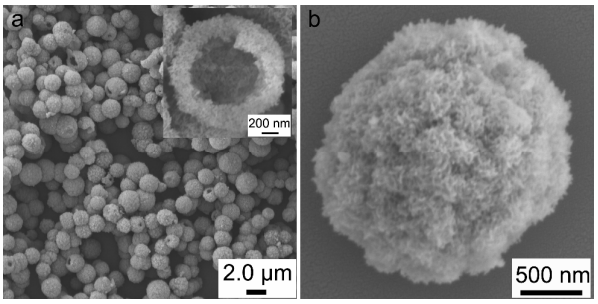

Figure S1. The SEM (a-b) images of the initial zinc citrate hollow microspheres. The inset in (a) shows a broken microsphere.

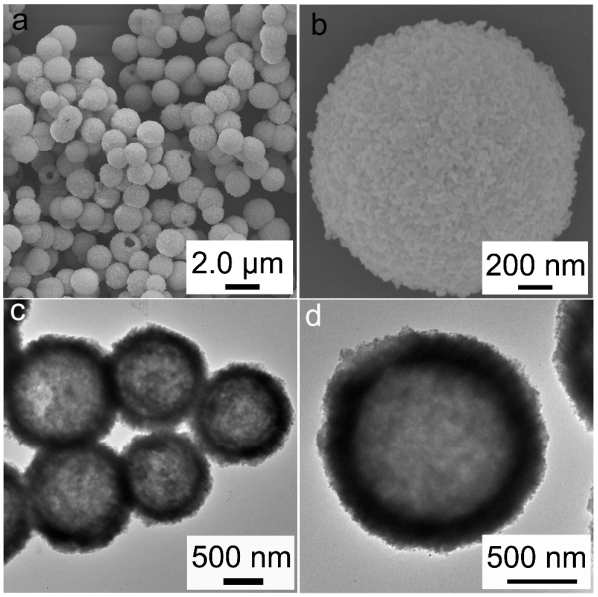

Figure S2. The SEM (a-b) and TEM (c-d) micrographs of zinc-silver citrate hollow microspheres.

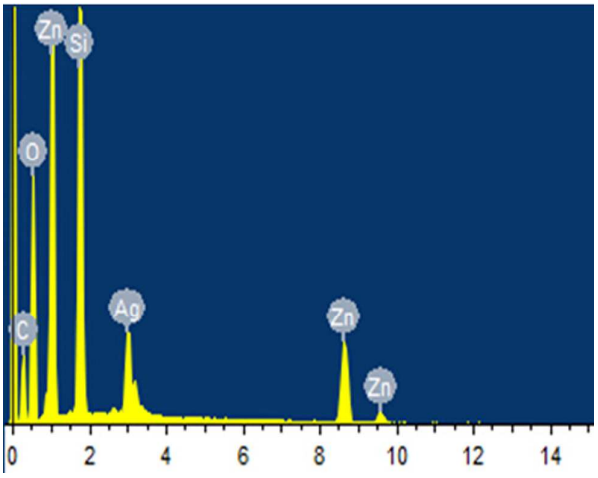

Figure S3. The EDS spectrum of zinc-silver citrate hollow microspheres. The Si signal comes from substrates.

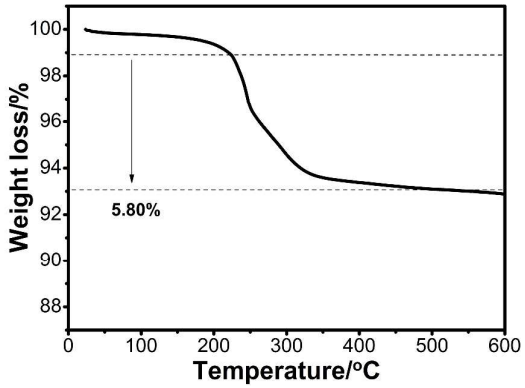

Figure S4. The TG investigation of sandwich-like Ag-C@ZnO-C@Ag-C hybrid hollow microspheres to determine the carbon content.

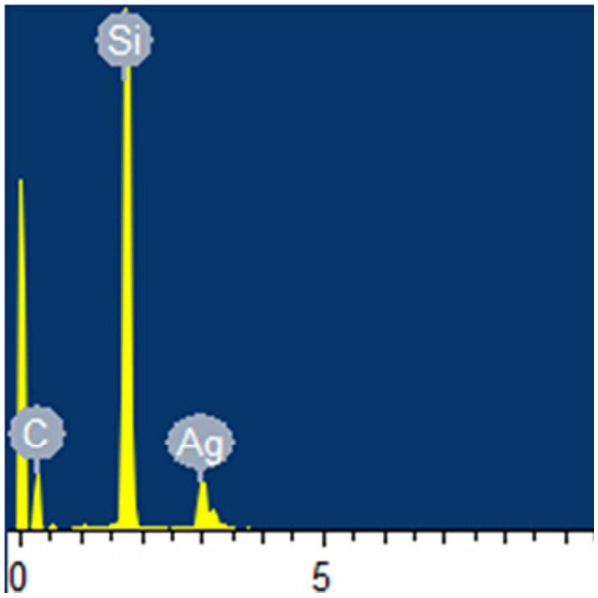

Figure S5. The EDS spectrum of double-shelled Ag-C hollow microspheres. The Si signal comes from substrates.

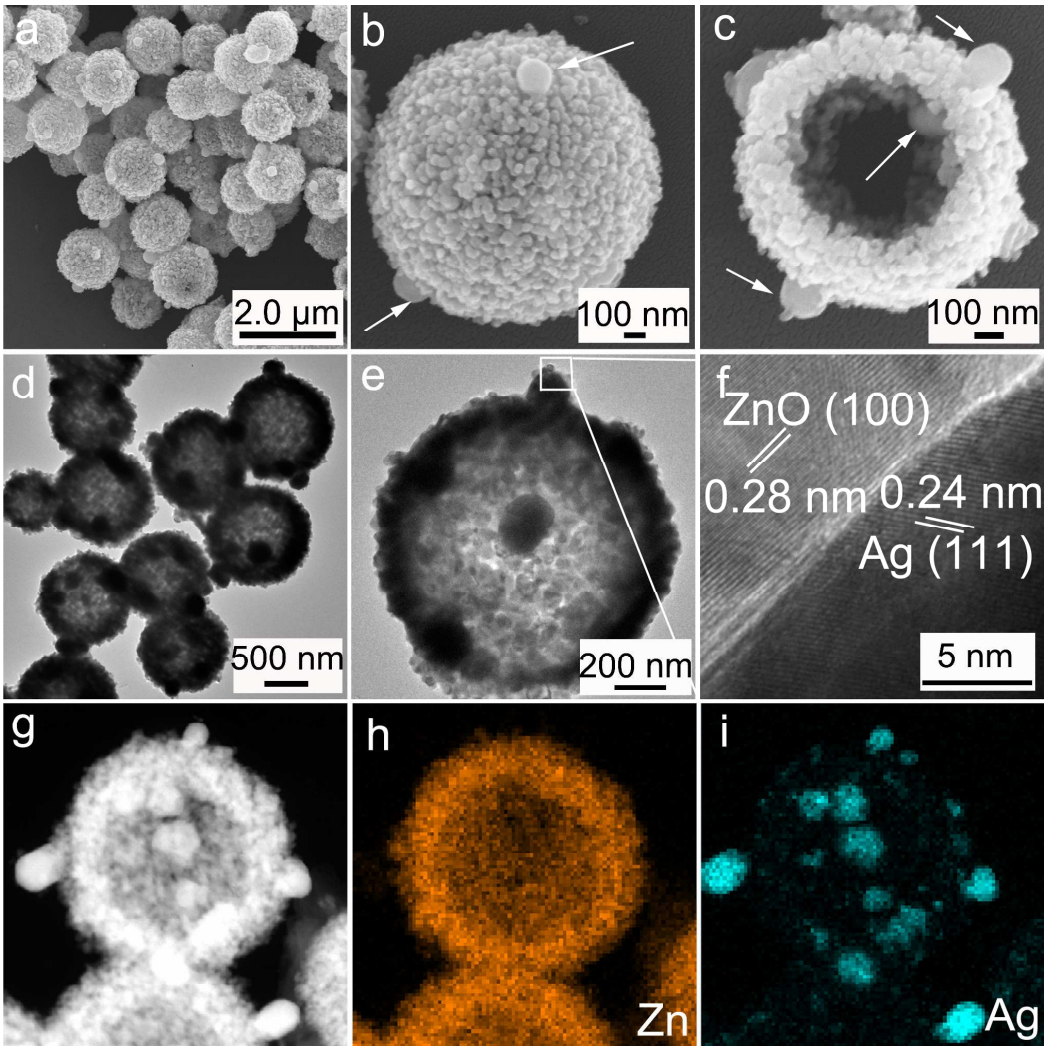

Figure S6. The SEM (a-c), TEM (d-e) and HRTEM (f) micrographs of ZnO/Ag hybrid hollow microspheres gained by calcination of zinc-silver citrate hollow microspheres in air. STEM image (g) and the dot-mapping images of Zn (h) and Ag (i).

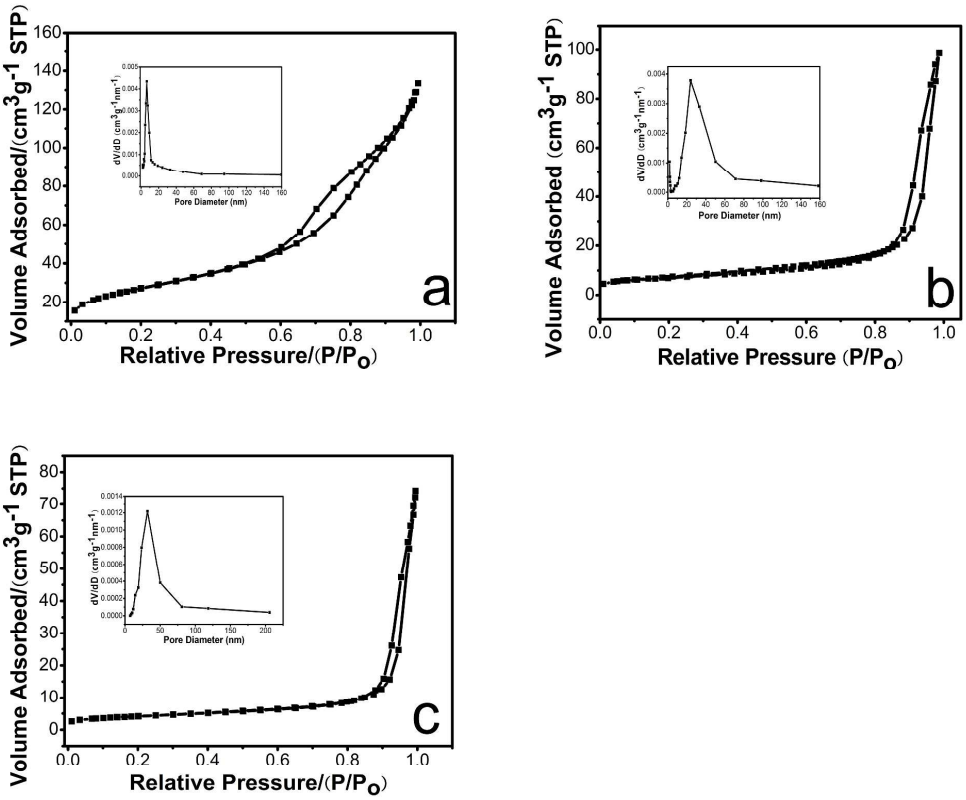

Figure S7. N_2 adsorption-desorption isotherms of Ag-C@ZnO-C@Ag-C (a), ZnO/Ag (b) and ZnO (c) hollow microspheres. The insets show the corresponding pore size distributions.

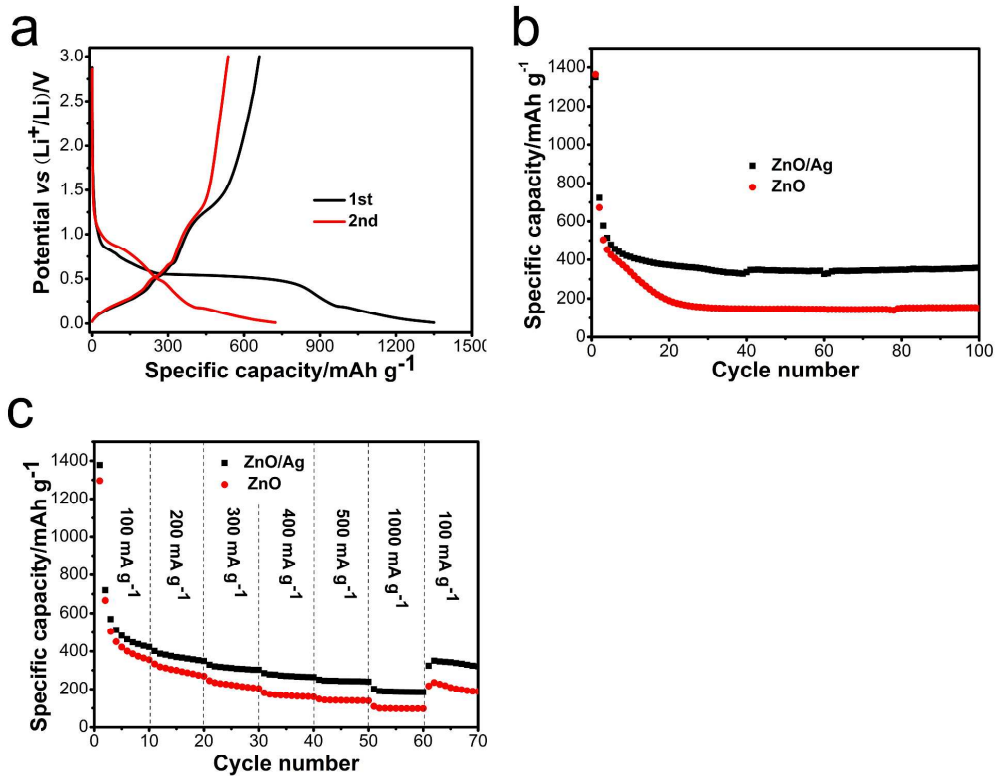

Figure S8. (a) The galvanostatic discharge-charge profiles of ZnO/Ag hybrid hollow microspheres. The cycling properties (b) at a current density of 100 mA g^{-1} and rate capabilities (c) of ZnO/Ag and ZnO hollow microspheres.

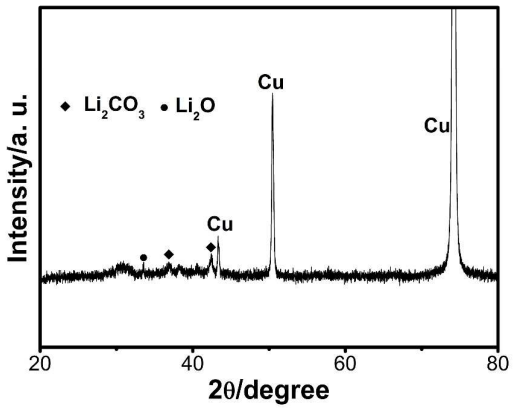

Figure S9. Ex situ XRD pattern of sandwich-like Ag-C@ZnO-C@Ag-C hybrid

hollow microsphere electrode after 200 cycles.

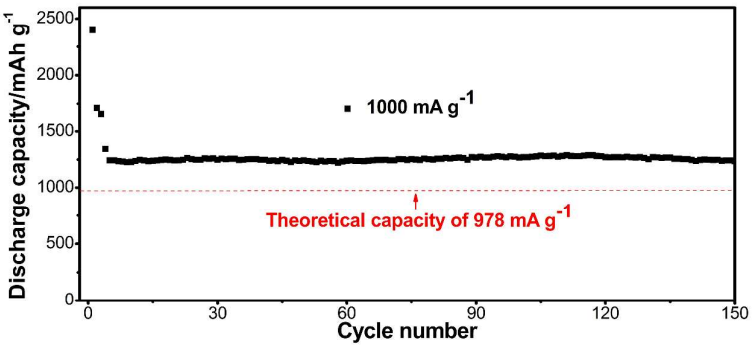

Figure S10. Cycling performances of sandwich-like Ag-C@ZnO-C@Ag-C hybrid hollow microsphere at 100 mA g^{-1} in the first three cycles and at 1000 mA g^{-1} in the following cycles.

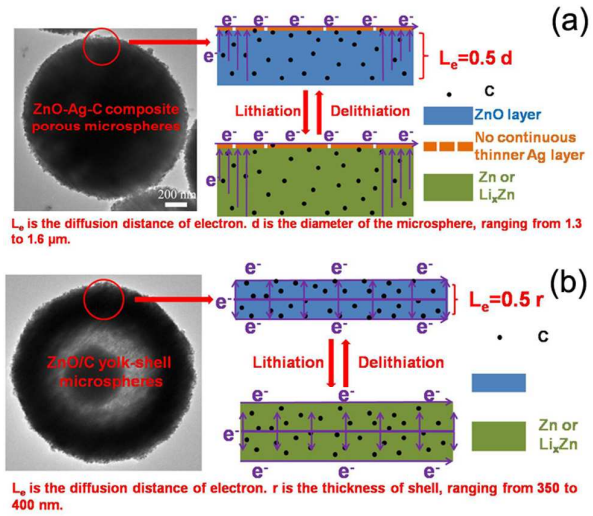

Figure S11. Schematic illustrations of electron transport process during cycling for ZnO-Ag-C composite porous microspheres (a) and yolk-shell ZnO-C hollow microspheres (b).

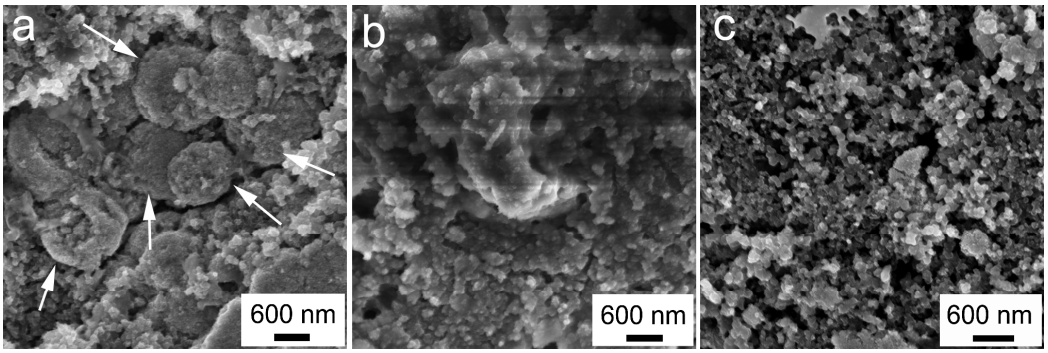

Figure S12. The SEM images of Ag-C@ZnO-C@Ag-C (a), ZnO/Ag (b) and ZnO (c) hollow microspheres after 100 cycles. The arrows indicate the intact microspheres.

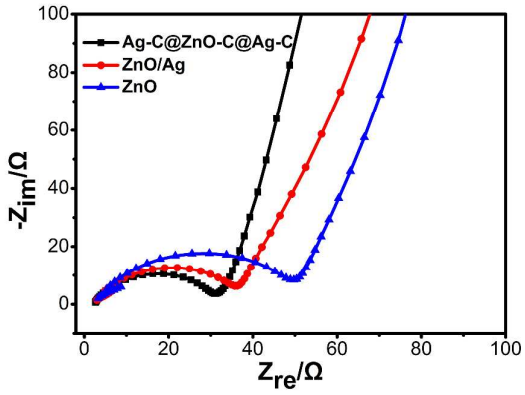

Figure S13. The electrochemical impedance spectroscopy of Ag-C@ZnO-C@Ag-C, ZnO/Ag and ZnO hollow microspheres before cycling.